

1

20

University of Houston Interlibrary Loan
ILLiad TN: 127612



Borrower: IQU

Lending String: *TXH,NTE,ORE,WYU,UUM

Patron: Coutσίας, Evangelos

Journal Title: Geophysical and astrophysical fluid dynamics.

Volume: 92 **Issue:** 1-2

Month/Year: 2000 **Pages:** 85-114

Article Author:

Article Title: vande Konijnenberg, Naulin, Rasmussen, Stenum, vanHeijst; Linear spin-up in a sliced cylinder

NOTES:

ILL Number: 9068776



This material may be protected by copyright law (Title 17, U.S. Code)

Call #: QC809.F5 G4

Location: 3 GOLD

Shipping Address:
IQU-Zimmerman Library ILL
1 University of New Mexico
MSC05 3020
One University of New Mexico
Albuquerque, NM 87131-0001

Fax:
Ariel: 129.24.209.172

ILL Office Hours: Monday - Friday, 8am - 5pm
Phone: (713) 743-9720
FAX: (713) 743-9725
E-Mail: ill@lib.uh.edu
<http://info.lib.uh.edu/services/illpol.html>

LINEAR SPIN-UP IN A SLICED CYLINDER

J. A. VAN DE KONIJNENBERG^a, V. NAULIN^a,
J. JUUL RASMUSSEN^a, B. STENUM^{a,*}
and G. J. F. VAN HEIJST^b

^a*Riso National Laboratory, Optics and Fluid Dynamics Department,
Building 128, P.O. Box 49, 4000 Roskilde, Denmark;*

^b*Fluid Dynamics Laboratory, Department of Technical Physics,
Eindhoven University of Technology, P.O. Box 513,
5600 MB Eindhoven, The Netherlands*

(Received 11 May 1999; In final form 13 December 1999)

Spin-up and spin-down in a circular tank with a uniformly sloping bottom are studied experimentally and numerically for small values of the relative change in the angular velocity of the tank. Generally, the initial single-cell flow evolves into a number of smaller vortices. The evolution is compared with an analytical model based on an expansion of the flow field in linear Rossby waves (Pedlosky and Greenspan, 1967). Although it is possible to tune the experimental parameters in such a way that agreement with the theory is found, in most cases the experiments show shedding of vortices in the initial stage of the spin-up or spin-down, a phenomenon not described by the analytical model. Nonetheless, in such cases the analytical model still accounts for other observations: the alternating generation of cyclonic and anticyclonic vortices in the eastern part of the tank and their subsequent westward motion.

Keywords: Spin-up; β -plane; sliced cylinder

1. INTRODUCTION

During the last decades, the spin-up of a homogeneous fluid to a final state of solid-body rotation due to a change in the angular velocity of its container has received considerable attention. Most studies on this

*Corresponding author. e-mail: bjarne.stenum@tisoedk

subject concerned the flow in a circular tank (Greenspan and Howard, 1963; Wedemeyer, 1964; Weidman, 1976; Van de Konijnenberg and Van Heijst, 1995). In a circular geometry, the flow remains approximately azimuthal, and slowly gains a higher angular velocity by a secondary flow driven by the Ekman layers at the bottom and, if present, at the lid of the tank. Van Heijst (1989) first studied spin-up in cylindrical geometries with non-circular cross section, such as a semi-circle and a circle with a radial barrier. This study was followed by a number of publications on spin-up in various geometries, most of them rectangular (Van Heijst *et al.*, 1990; Van Heijst *et al.*, 1994; Suh, 1994; Van de Konijnenberg, 1995). In non-circular geometries, the flow usually separates from the lateral boundaries, and evolves into a pattern of a small number of counterrotating vortices. The organization into a quasi-steady streamline pattern depends on experimental parameters such as the shape of the container and the angular velocity. Geometries that can accommodate a small number of equally-sized vortices, such as a slender rectangular tank, favour the formation of a quasi-steady vortex pattern. The occurrence of self-organization in spin-up experiments is related to the two-dimensional nature of rotating flows. Spin-up flows are not only approximately horizontal, but also independent of the vertical coordinate. However, the presence of Ekman layers leads to differences from purely two-dimensional flows, in particular with respect to the decay of the relative flow.

A different class of non-axisymmetric geometries is formed by the introduction of a sloping bottom. Already in 1967, Pedlosky and Greenspan studied spin-up in a sliced cylinder – a circular cylinder with a uniformly sloping bottom and a flat rigid lid. Pedlosky and Greenspan presented an analytical solution for the time-dependent flow for the case in which the increase in angular velocity is very small. This solution consists of an expansion in Rossby wave modes, multiplied by an overall factor representing the exponential decay of the relative flow due to Ekman pumping.

Van Heijst *et al.* (1994) combined a rectangular geometry with a sloping bottom. In this case the flow tends to become very complicated and erratic; usually there is no formation of a quasi-steady streamline pattern. In late stages of the evolution it should be possible to describe the flow in terms of linear Rossby waves, but unless the relative increase in angular velocity is small compared with the relative

differences in depth, separation from the sidewall and vortex formation takes place in the interior.

In the present paper we study the spin-up in a tank with a uniformly sloping bottom. This geometry is a natural extension of axisymmetric flow in the limiting case of a flat bottom, so that the effect of the topography is small. The present work will show that also in this case, flow separation from the sidewall is the rule rather than the exception.

The study of the flow in a tank with a sloping bottom is relevant for meso-scale flows in the Earth's oceans. The effect of non-uniform depth acts in a similar way to the effect of the Coriolis parameter f . Indeed, in subsequent papers by Beardsley and Greenspan (1985) and in subsequent papers by Beardsley and Robbins (1975) the sliced cylinder model is used to study ocean circulation. The emphasis of these papers is on the flow with stationary forcing by a difference in depth. In the present paper we study the spin-up in a tank with a sloping bottom, at the modelling of a particular aspect of the flow.

The further organisation of this paper is as follows. The aspects of the spin-up flow in the tank are reviewed in Sect. 2. The linear theory is derived in Sect. 3. Numerical methods are explained in Sect. 4. The numerical results are presented in Sect. 6 and compared with the analytical results by the numerical results in Sect. 8. Conclusions are drawn in Sect. 9.

2. GENERAL BACKGROUND

Three dimensionless parameters describe the flow in this paper. The first one is the Rossby number, in general, a measure of the relative importance of the ground rotation. In the present paper it is defined as $\Delta\Omega/\Omega$, the increase in angular velocity divided by the angular velocity. We will restrict ourselves to Rossby numbers between -0.1 and 0.1 . The second parameter is the Ekman number, defined as $\nu/(\Omega H^2)$, with ν the kinematic viscosity and H the depth in the tank. The third parameter is the relative depth difference between the depth difference ΔH and the mean depth H .

circular tank (Greenspan and Howard, 1976; Van de Konijnenberg and Greenspan, 1976). In a circular geometry, the flow remains approximately uniform and slowly gains a higher angular velocity by Ekman pumping at the bottom and, if the Ekman layers are thin, by the Ekman layers at the top. Van Heijst (1989) first studied spin-up in a circular tank with a non-circular cross section, such as a rectangular tank with a radial barrier. This study was followed by Van Heijst *et al.* (1990) and Van Heijst *et al.* (1994). In non-circular geometries, the flow separates from the lateral boundaries, and evolves into a pattern of counterrotating vortices. The number of vortices depends on the shape of the container and the depth. A rectangular tank can accommodate a small number of vortices, while a slender rectangular tank, favouring a single vortex pattern. The occurrence of self-organising vortices is related to the two-dimensional nature of the flow. Spin-up flows are not only approximately uniform in the vertical coordinate. However, the presence of Ekman layers leads to differences from purely two-dimensional flow with respect to the decay of the

symmetric geometries is formed by the Ekman pumping. Already in 1967, Pedlosky and Greenspan studied a sliced cylinder – a circular cylinder with a sloping bottom and a flat rigid lid. Pedlosky and Greenspan (1967) found an analytical solution for the time-dependent increase in angular velocity is very similar to that of an expansion in Rossby wave number, with a factor representing the exponential Ekman pumping.

When combined a rectangular geometry with a sloping bottom, the flow tends to become very complicated. The formation of a quasi-steady streamfunction and the evolution it should be possible to predict in terms of Rossby waves, but unless the relative depth difference is small compared with the relative

differences in depth, separation from the sidewall and subsequent vortex formation takes place in the beginning of the experiment.

In the present paper we study the spin-up in a circular tank with a uniformly sloping bottom. This geometry has the attractive property of axisymmetric flow in the limiting case of a vanishing topography, so that the effect of the topography becomes particularly clear. We will show that also in this case, flow separation and vortex shedding from the sidewall is the rule rather than the exception.

The study of the flow in a tank with a sloping bottom has relevance for meso-scale flows in the Earth's atmosphere and oceans, since the non-uniform depth acts in a similar way as a latitudinal variation in the Coriolis parameter f . Indeed, in Pedlosky and Greenspan (1967) and in subsequent papers by Beardsley (1969) and Beardsley and Robbins (1975) the sliced cylinder had the purpose of modelling the ocean circulation. The emphasis of those papers, however, is on flows with stationary forcing by a differential rotation of the rigid lid. In the present paper we study the spin-up process without aiming directly at the modelling of a particular geophysical flow.

The further organisation of this paper is as follows. Some general aspects of the spin-up flow in the geometry under consideration are reviewed in Sect. 2. The linear theory and the experimental and numerical methods are explained in Sects. 3, 4 and 5. The experimental results are presented in Sect. 6 and discussed in Sect. 7, to be followed by the numerical results in Sect. 8. Finally, some general conclusions are drawn in Sect. 9.

2. GENERAL BACKGROUND

Three dimensionless parameters determine the spin-up we consider in this paper. The first one is the Rossby number Ro , which is, in general, a measure of the relative flow with respect to the background rotation. In the present paper we define it as $Ro = \Delta\Omega/\Omega$, with $\Delta\Omega$ the increase in angular velocity and Ω the final angular velocity. We will restrict ourselves to Rossby numbers in the range between -0.1 and 0.1 . The second parameter is the Ekman number E , defined as $\nu/(\Omega H^2)$, with ν the kinematic viscosity and H a measure of the depth in the tank. The third parameter is $\kappa = \Delta H/H_{\max}$, the ratio between the depth difference $\Delta H = H_{\max} - H_{\min}$ between the deepest

and the shallowest part, and the maximum depth. It is this parameter which gives rise to differences from earlier studies on spin-up in a circular tank with a flat bottom. A fourth parameter would be the ratio between depth H_{\max} and radius a of the tank, but in the present paper both H_{\max} and a are fixed.

It is well known that an inclined bottom influences a rotating fluid by vortex stretching, in a way that leads to similar dynamics as in the β -plane model of meso-scale geophysical flow (see e.g., Van Heijst, 1994). Summarizing the essential points, the flow of fluid along a depth gradient leads to an increase of vorticity ω given for small Rossby number by $\partial\omega/\partial t = 2\Omega H^{-1} \mathbf{v} \cdot \nabla H$, where \mathbf{v} is the horizontal velocity field. With the depth gradient taken in the negative y -direction, this can be written as $\partial\omega/\partial t = -\beta v_y$, with $\beta = -2\Omega H^{-1} \partial H/\partial y$. In a geophysical context, one finds the same term $-\beta v_y$, but with $\beta = 2\Omega \cos\phi/R$, with ϕ the latitude and R the Earth's radius. In view of this analogy, the shallow part of the tank is referred to as the north, and the deeper part as the south. In this paper we take the x - and y -direction in the direction of the east resp. the north, the origin coinciding with the centre of the tank.

According to both the topographic and geophysical definition, the parameter β is a local quantity. However, it is common practice to use the β -plane model, in which β is uniform throughout the domain under consideration. In a sliced cylinder this is never quite true, since the depth is not uniform. [A uniform value for β could be obtained by a depth of the form $H(y) = c_1 \exp(y/c_2)$, but this is not a geometry we used in our experiments.] The question naturally arises what value for H should be chosen if the sliced cylinder is to be represented by a β -plane. In the present paper we adopted the central value $H(0) = (1/2)(H_{\max} + H_{\min})$, representing an average of the depth over the area of the tank. Although arbitrary to a certain extent, this choice provides a reasonable average between the extreme values H_{\max} and H_{\min} . Note that the same question appears in the definition of the Ekman number; also in that case we choose the average depth $H(0)$.

In the experiments, the rotation of the flow does not only give rise to the topographic β -effect, but also to the formation of Ekman layers at the bottom and top of the vessel. The Ekman layers lead to a secondary flow, which ultimately leads to the decay of the relative flow. The secondary flow leads to a contraction or dilatation of the

two-dimensional velocity field, so that the three-dimensional divergence $\nabla \cdot \mathbf{v}$. If both the Ekman number and the Rossby number are small, $\nabla \cdot \mathbf{v}$ may be neglected. $\lambda = 2\sqrt{\nu\Omega}/H$ is the inverse of the Ekman number (Howard, 1963). Making this assumption, the vorticity equation becomes

$$\frac{\partial\omega}{\partial t} + \mathbf{v} \cdot \nabla\omega + \beta v_y$$

This equation, together with the continuity equation for the three-dimensional velocity field is divergent, and is not suitable for numerical simulation.

More generally, the smallness of the Ekman number is exploited with different theoretical models, sometimes categorized as 'linear'. In the present paper, $\nabla \cdot \mathbf{v} = \lambda\omega$, so the two-dimensional velocity field and the Ekman suction is proportional to the vorticity. In the 'compressible' (i.e., not incompressible) vorticity equation, this corresponds to a non-linear spin-up in a circular cylinder. In the β -plane model, the vorticity equation becomes

$$\frac{\partial\omega}{\partial t} + \mathbf{v} \cdot \nabla\omega + \beta(1 + \omega/2\Omega)v_y$$

where also the β -term is given in terms of the depth. In the present paper we use this form of the vorticity equation in our discussions only. Second, one may neglect the Ekman suction in addition to the assumption of incompressibility, which reminds of the Boussinesq approximation for small density fluctuations, and means that the continuity equation is neglected, except in the Ekman layers. The continuity equation is replaced by $\lambda\omega$. It can be shown that this is a good approximation in the present model (i.e., one in which the Ekman number is small, the domain remains zero), the two-dimensional velocity field is replaced by 1. Thus, this assumption of incompressibility of the two-dimensional flow is equivalent to the Boussinesq approximation of the β -term and the Ekman-damping.

the maximum depth. It is this parameter from earlier studies on spin-up in a tank. A fourth parameter would be the radius a of the tank, but in the present study it is neglected.

An inclined bottom influences a rotating fluid in a way that leads to similar dynamics as in the case of geophysical flow (see e.g., Van Heijst, 1994). At certain points, the flow of fluid along a slope leads to an increase of vorticity ω given for small $H^{-1}\mathbf{v} \cdot \nabla H$, where \mathbf{v} is the horizontal velocity. The gradient taken in the negative y -direction, $\partial/\partial y = -\beta v_y$, with $\beta = -2\Omega H^{-1}\partial H/\partial y$. In the case of a sphere one finds the same term $-\beta v_y$, but with $\beta = 2/R$, where R is the Earth's radius. In view of the fact that the part of the tank is referred to as the 'south' pole, in this paper we take the x -axis pointing towards the east resp. the north, the y -axis towards the south of the tank.

In a geographic and geophysical definition, the depth H is not uniform. However, it is common practice to use a constant value for H throughout the domain. In a cylindrical tank this is never quite true, since H is not uniform. A uniform value for β could be obtained if $H = H_0 \exp(y/c_2)$, but this is not a geometry of a sliced cylinder. The question naturally arises what value for H in the sliced cylinder is to be represented. In this paper we adopted the central value $H(0)$ representing an average of the depth over the domain. In an arbitrary to a certain extent, this choice is made between the extreme values H_{\max} and H_{\min} . The choice appears in the definition of the vorticity ω . If we choose the average depth $H(0)$, the velocity field of the flow does not only give rise to Ekman layers, but also to the formation of Ekman layers in the vessel. The Ekman layers lead to a contraction or dilatation of the

two-dimensional velocity field, so it can be represented by the two-dimensional divergence $\nabla \cdot \mathbf{v}$. If both the Rossby number and the Ekman number are small, $\nabla \cdot \mathbf{v}$ may be approximated by $\lambda\omega$, where $\lambda = 2\sqrt{\nu\Omega}/H$ is the inverse of the spin-up time (see Greenspan and Howard, 1963). Making this assumption and including the β -term, the vorticity equation becomes

$$\frac{\partial\omega}{\partial t} + \mathbf{v} \cdot \nabla\omega + \beta v_y = -\lambda\omega + \nu\nabla^2\omega. \quad (1)$$

This equation, together with the approximation that the two-dimensional velocity field is divergence-free, was used in the numerical simulation.

More generally, the smallness of the Rossby number may be exploited with different theoretical assumptions, all of which are sometimes categorized as 'linear'. First, one may assume that in every point, $\nabla \cdot \mathbf{v} = \lambda\omega$, so the two-dimensional divergence resulting from the Ekman suction is proportional to the relative vorticity. Combined with the 'compressible' (i.e., not divergence-free) two-dimensional vorticity equation, this corresponds to the Wedemeyer model in non-linear spin-up in a circular cylinder (Wedemeyer, 1964). With this model, the vorticity equation becomes

$$\frac{\partial\omega}{\partial t} + \mathbf{v} \cdot \nabla\omega + \beta(1 + \omega/2\Omega)v_y = -\lambda(1 + \omega/2\Omega)\omega + \nu\nabla^2\omega, \quad (2)$$

where also the β -term is given in its 'compressible' form. In the present paper we use this form of the vorticity equation for qualitative discussions only. Second, one may consider the velocity field as solenoidal in addition to the assumption that $\nabla \cdot \mathbf{v} = \lambda\omega$. This approach reminds of the Boussinesq approximation for flow with density fluctuations, and means that the divergent part of the velocity field is neglected, except in the Ekman damping term where the divergence is replaced by $\lambda\omega$. It can be shown that in order to obtain a consistent model (i.e., one in which the vorticity integrated over the entire domain remains zero), the two factors $1 + \omega/2\Omega$ in (2) should be replaced by 1. Thus, this assumption leads to (1); the incompressibility of the two-dimensional flow is explicitly visible from the form of the β -term and the Ekman-damping term, and implicitly taken into

account in the advective term. Third, one may also neglect the advective term. This assumption is quite drastic, since it eliminates the possibility of vortex shedding from domain boundaries; in fact, it eliminates the very existence of vortices in the way they are usually interpreted. In reality, advection of vorticity tends to be important even if the Rossby number is small. Indeed, in the absence of the β -effect and (more hypothetically) Ekman suction, the influence of the background rotation is not noticeable at all, so the advective term plays the same role as in a non-rotating fluid. We will show that in our experiments with the Rossby number of the order of 0.1, the advective term cannot be neglected.

3. LINEAR THEORY

An analytical expression to the linear spin-up problem in the limiting case $Ro \rightarrow 0$ was given by Pedlosky and Greenspan (1967). Their result is a solution of (1) with the omission of the advective term, the Ekman damping term and the viscous term. There seems to be little need to review the method they used (for more explanation the reader may also consult Pedlosky, 1987). However, the result of Pedlosky and Greenspan seems to include a typographical error with respect to the time-dependent terms. We repeated the calculation and arrived (in dimensional quantities) at

$$\frac{\psi(x, y, t)}{\Delta\Omega a^2} = - \sum_{m=0}^{\infty} \sum_{n=1}^{\infty} \frac{4\delta_m}{k_{mn}^2} J_m\left(\frac{k_{mn}r}{a}\right) \cos(m\theta) \cos\left(\frac{k_{mn}x}{a} + \frac{\beta at}{2k_{mn}} - \frac{m\pi}{2}\right) \quad (3)$$

or, with faster convergence,

$$\frac{\psi(x, y, t)}{\Delta\Omega a^2} = \frac{1}{2} \left(\frac{r^2}{a^2} - 1 \right) + \sum_{m=0}^{\infty} \sum_{n=1}^{\infty} \frac{8\delta_m}{k_{mn}^2} J_m\left(\frac{k_{mn}r}{a}\right) \cos(m\theta) \sin\left(\frac{k_{mn}x}{a} + \frac{\beta at}{4k_{mn}} - \frac{m\pi}{2}\right) \sin\left(\frac{\beta at}{4k_{mn}}\right) \quad (4)$$

with ψ the stream function, and k_{mn} the n th order Bessel function, $\delta_0 = 1/2$, and $\delta_m = 1$ for $m > 0$. In translation of symbols, this corresponds to Greenspan (1968).

Each mode is characterized by a set of azimuthal nodal lines, intersected by radial nodal lines north-south and moving from east to west up to a solid-body rotation. However, with increasing velocity, the coherence of the initial vortices ($\beta at = 5.68$, the first invading vortex) is destroyed, the tank, replacing the initial anti-cyclonic vortices and smaller structures appear as a result of an overview of the first stages of the flow (see figure 1 to $\beta at = 48$).

4. EXPERIMENTAL SET-UP

The experiments were performed in a tank with $a = 20$ cm, depth $H_{\max} = 20$ cm and a horizontal β -plane was created with a thin elliptic plate designed for a particular experiment. The tank was placed on a rotating table, seeded with small ($\sim 50 \mu\text{m}$) particles, and the rigid lid, so there is no free surface. The rotation of the table was changed in a few seconds, a period of a few seconds is compared with the spin-up time of the tank, but short compared with the time scale of the flow in the rotating system. The angular velocity Ω was always equal to 2.0 rad/s. The data were collected electronically, and are accurate to 1%. The flow patterns obtained by intersecting the tank with a laser sheet, applying tracking techniques to the particles, and video recording of the flow was monitored with the tank. Then, after the experiment, the data were processed by a PC equipped with a frame grabber and an image system developed by Dalgaard (1995). The image processing system that allows

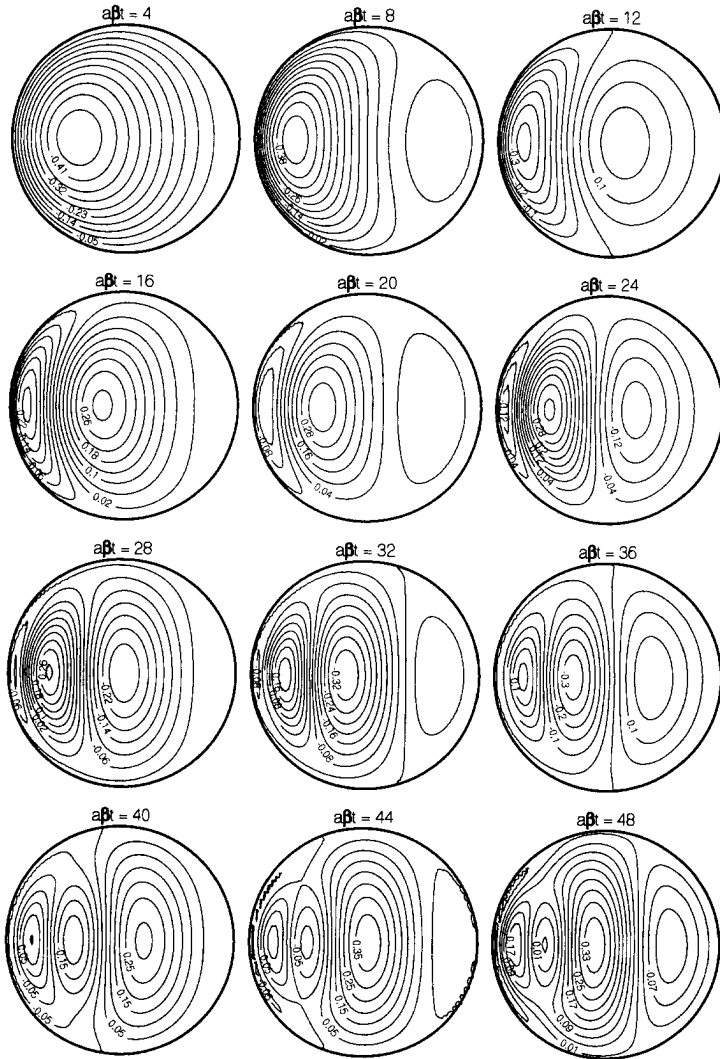


FIGURE 1 Stream function of the spin-up flow according to the analytical solution. The numbers at the contours are the values of $\psi/\Delta\Omega a^2$. In all figures in the present paper, the depth increases in the direction from the top to the bottom of the page. (This means that the positive x -direction is to the right, the positive y -direction to the top of the page.) A positive value of the stream function corresponds to a cyclonic rotation.

on a number of user-defined criteria such as brightness and size. The vorticity was obtained by matching the data with spline functions and manipulating the coefficients of this expansion. The stream

TABLE I Overview of

	$Ro = \Delta\Omega/\Omega$	$\kappa = \Delta H$
Experiment 1	0.01	0.
Experiment 2	0.1	0.
Experiment 3	-0.1	0.
Experiment 4	0.1	0.

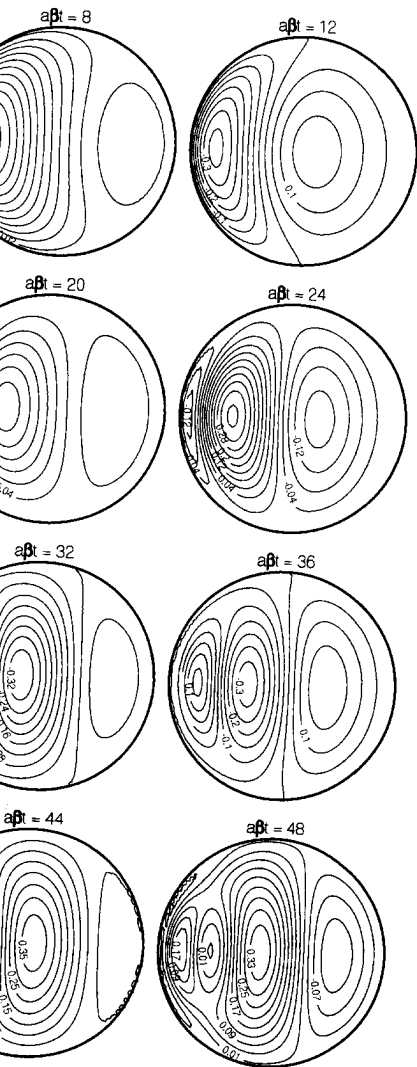
function was calculated from the v. In this way the stream function of velocity field is calculated (not, a option, the stream function based the local depth).

In addition to the experiments performed with a small amount of water. In this way, a qualitative im obtained. In particular, these visual sional instabilities develop at the: tually two-dimensional. The absence different depths is so convincing less to perform measurements with

Four experiments are described values for the Rossby number (see a comparison with the analytical t conditions leading to agreement laxed, and vortex shedding from. These experiments form the backl they demonstrate the phenomena clarifies the crucial role of the ratio

5. NUMERICAL METHOD

In order to make a comparison w lated a numerical solution of (1) to experiment 2 (see Tab. I). F difference method in the vorticity this method the flow is assumed though the dynamical consequen ing (induced by the topography a account, the contraction or dilata



spin-up flow according to the analytical solution. The values of $\psi/\Delta\Omega\alpha^2$. In all figures in the present paper, the positive y -direction is from the top to the bottom of the page. (This is the opposite to the convention in the right, the positive y -direction to the top of the page. The stream function corresponds to a cyclonic rotation.

criteria such as brightness and size. The data with spline functions of this expansion. The stream

TABLE I Overview of experimental parameters

	$Ro = \Delta\Omega/\Omega$	$\kappa = \Delta H/H_{max}$	$\beta (m^{-1}s^{-1})$	E
Experiment 1	0.01	0.5	6.66	2.22×10^{-5}
Experiment 2	0.1	0.1	1.05	1.39×10^{-5}
Experiment 3	-0.1	0.1	1.05	1.39×10^{-5}
Experiment 4	0.1	0.5	6.66	2.22×10^{-5}

function was calculated from the vorticity by using a Poisson solver. In this way the stream function of the solenoidal component of the velocity field is calculated (not, as would have been an alternative option, the stream function based on a velocity field weighted with the local depth).

In addition to the experiments with particles, experiments were performed with a small amount of dye added to the otherwise clear water. In this way, a qualitative impression of the flow field could be obtained. In particular, these visualizations show that no three-dimensional instabilities develop at the sidewall, and the flow remains virtually two-dimensional. The absence of differential advection of dye at different depths is so convincing that we considered it to be pointless to perform measurements with light sheets at varying depth.

Four experiments are described in the present paper, all with small values for the Rossby number (see Tab. I). Experiment 1 is aimed at a comparison with the analytical theory. In experiments 2 and 3, the conditions leading to agreement with the analytical theory are relaxed, and vortex shedding from the sidewall is seen to take place. These experiments form the backbone of the paper, in the sense that they demonstrate the phenomena we wish to describe. Experiment 4 clarifies the crucial role of the ratio Ro/κ in experiments of this type.

5. NUMERICAL METHOD

In order to make a comparison with the experimental data, we calculated a numerical solution of (1) with the parameters corresponding to experiment 2 (see Tab. I). For this purpose we used a finite-difference method in the vorticity, stream-function formulation. In this method the flow is assumed to be strictly incompressible, so although the dynamical consequences of vortex stretching and squeezing (induced by the topography and the Ekman layers) are taken into account, the contraction or dilatation itself is neglected. The numerical

scheme utilizes a third-order stiffly stable time-stepping algorithm as described by Karniadakis *et al.* (1991). The diffusive term is treated implicitly, and the circular domain discretized in polar co-ordinates. The use of a staggered grid – i.e., the n grid-points are located at the centres of the n boxes filling the domain, rather than on the edges of the boxes – in the radial direction avoids the need for a special treatment of the co-ordinate singularity at $r=0$. Grid-points were spaced non-equidistantly in the radial direction; a cosine distribution was used across the diameter to have a higher spatial resolution near the wall, where steep gradients appear due to the no-slip boundary condition. The no-slip boundary condition was implemented by adjusting the vorticity at $r=a$ so that the normal derivative of the stream function vanishes. Additionally, in the implicit viscous solver an artificially high value for the viscosity at $r=a$ was used, so that on the outermost grid-points the vorticity was coupled strongly to the vorticity on the wall. In the solution of the Poisson equation, the stream function was taken to be zero at $r=a$. The advective term has the form of a Poisson bracket, and was calculated using the discretized form given by Arakawa (1966). This discretization retains the most important symmetries of the advection term, that is, conservation of energy and enstrophy. The numerical scheme was verified by reproducing the results of the spectral code described in Coutsis and Lynov (1991) for the case of a Lamb dipole impinging on a no-slip wall, while the regularity of the centre was checked by monitoring a Lamb dipole moving through it. No spurious effects were noticed at the co-ordinate origin in that case.

For the initial condition we assume that immediately after a change $\Delta\Omega$ in the angular velocity, the absolute vorticity in the non-rotating system is still unaffected by the motion of the sidewalls. As a result, the relative vorticity of the starting flow has a uniform value $-2\Delta\Omega$. However, at the sidewall, the no-slip boundary condition gives rise to a singular layer of concentrated vorticity with positive sign. This shear layer starts to thicken by viscous diffusion immediately after its formation, but the start of the experiment may be considered as the limiting case in which this shear layer is singular. The velocity field of this initial condition, referred to as the starting flow, is determined by

$$\nabla \times \mathbf{u} = -2\Delta\Omega \quad (5)$$

with zero normal velocity at all sides. For a circular geometry with a flat bottom and a rigid body rotation with angular velocity Ω , the starting flow, however, an analytic solution is not available. An approximation for the starting flow was given by Van de Konijnenberg (1991). For a rotation αa , this result implies a displacement of the vortex by $(3/8)\alpha a$ to the deeper part of the tank. For a rotation ΔH of 2 cm, a depth H of 20 cm yields 0.375 cm. In view of its small magnitude, it was ignored in the initial condition of the present study. Body rotation has been used instead of a rigid body rotation.

The representation of the sloped bottom in the numerical model requires further investigation. An argument that can be found in Pridmore (1991) is that the pumping velocity for a layer of fluid of thickness $(1/2)(\nu/\Omega)^{1/2}(\cos\alpha)^{-1/2}\omega$ in the non-rotating case is reduced to a pumping velocity $(1/2)(\nu/\Omega)^{1/2}\omega$ in the rotating case. This means an increase of the pumping rate by a factor $\cos^{-3/2}\alpha$. The two-dimensional case is the sum of the pumping rates at all angles. For a rotation of 2.00 rad/s by the local depth of the fluid. For a rotation of 2.00 rad/s from 1 by less than 0.2%. In our case, the depth is taken into account. The depth difference is of the order of 10% in the local divergence. The results of the numerical run with the initial condition are investigated in further detail.

6. EXPERIMENTAL RESULTS

6.1. Experiment 1: Spin-up $Ro = 0$

Experiment 1 (with the angular velocity 2.00 rad/s and depth varying from 10 to 20 cm south) was performed in order to compare the experimental results with analytical results. The slope is 10% and the Rossby number has about the

stiffly stable time-stepping algorithm as *et al.* (1991). The diffusive term is treated on a domain discretized in polar co-ordinates. i.e., the n grid-points are located at the interior of the domain, rather than on the edges. This direction avoids the need for a special treatment of the singularity at $r=0$. Grid-points were distributed in the radial direction; a cosine distribution was used to have a higher spatial resolution near the walls. This appears due to the no-slip boundary condition. A boundary condition was implemented by adding a source term so that the normal derivative of the velocity is zero. Additionally, in the implicit viscous solver the viscosity at $r=a$ was used, so that the vorticity was coupled strongly to the solution of the Poisson equation, the vorticity is zero at $r=a$. The advective term was discretized, and was calculated using the discretization of *et al.* (1966). This discretization retains the conservation of the advection term, that is, conservation of vorticity. The numerical scheme was verified by comparing the results with a spectral code described in Coutias *et al.* (1991). The case of a Lamb dipole impinging on a cylinder was checked by monitoring the vorticity through it. No spurious effects were observed in that case.

Immediately after a change in the absolute vorticity in the non-rotating fluid, the motion of the sidewalls. As a result, the starting flow has a uniform value $-2\Delta\Omega$. The no-slip boundary condition gives rise to a boundary layer of vorticity with positive sign. This boundary layer is singular. The velocity field of the starting flow, is determined by

$$u = -2\Delta\Omega \quad (5)$$

with zero normal velocity at all solid boundaries. Clearly, for a circular geometry with a flat bottom, the solution consists of a solid-body rotation with angular velocity $-\Delta\Omega$. In the case of a sloping bottom, however, an analytic solution is difficult to construct. An approximation for the starting flow according to the shallow-water model was given by Van de Konijnenberg (1995). For small inclination α , this result implies a displacement of the centre of the starting vortex by $(3/8)\alpha a$ to the deeper part of the tank. For a bottom elevation ΔH of 2 cm, a depth H of 20 cm and a radius a of 20 cm, this yields 0.375 cm. In view of its smallness, this displacement has been ignored in the initial condition of the numerical simulation; a solid-body rotation has been used instead.

The representation of the sloping bottom by a two-dimensional numerical model requires further consideration. According to an argument that can be found in Pedlosky (1987), the Ekman pumping velocity for a layer of fluid with uniform inclination α is $(1/2)(\nu/\Omega)^{1/2}(\cos\alpha)^{-1/2}\omega$ in the normal direction, which corresponds to a pumping velocity $(1/2)(\nu/\Omega)^{1/2}(\cos\alpha)^{-3/2}\omega$ in the vertical direction. This means an increase of the bottom Ekman pumping rate by a factor $\cos^{-3/2}\alpha$. The two-dimensional divergence is then given by the sum of the pumping rates at the top and bottom plates, divided by the local depth of the fluid. For $\kappa=0.1$, the factor $\cos^{-3/2}\alpha$ differs from 1 by less than 0.2%. In our simulation, this correction was not taken into account. The depth differences lead to a larger error of the order of 10% in the local divergence, but in view of the success of the numerical run with the incompressible method, we did not investigate this matter in further detail.

6. EXPERIMENTAL RESULTS

6.1. Experiment 1: Spin-up $Ro = 0.01$, $\kappa = 0.5$

Experiment 1 (with the angular velocity increasing from 1.98 to 2.00 rad/s and depth varying from 10 cm in the north to 20 cm in the south) was performed in order to find an optimal agreement with the analytical results. The slope is very pronounced in this case, and the Rossby number has about the smallest value we could deal with.

Since the relative flow is very weak, the accuracy of these results is lower than that of the other experimental results in this paper. However, the stream function, being an integral over the velocity field that is actually measured, still gives acceptable results up to $\beta at = 48$. The results are presented in Figure 2. In spite of the Rossby number being small, its finite value is still noticeable. Around $\beta at = 20$, there is a slight asymmetry with respect to reflection in the x -axis. Experiments with varying $\Delta\Omega$ indicate that this is a result of the Rossby number still being too large. Moreover, at a closer look, the streamline pattern in the experiment seems to evolve slightly faster than the analytical theory predicts. However, this can be ascribed to the unprecise definition of the parameter β in the case of large depth differences (see Sect. 2). As the dimensionless time βat depends on β , the apparent speed of the evolution may easily be off by 10%.

The limited accuracy of this experiment does not allow a detailed quantitative comparison with the theory, but some observations with respect to the value of the stream function can be made. When time increases, the experimental flow becomes weaker than the theoretical solution. This is a consequence of the decay of the experimental flow due to Ekman damping. The spin-up time in this experiment is given in dimensionless time by $\beta a/\lambda = 70.7$. This means that at $\beta at = 48$, the experimental flow should have decayed by a factor $\exp(-48/70.7) = 0.507$. A comparison between the experimental and numerical results (taking into account a time lag $\beta a\Delta t \approx 4$) shows that this is roughly correct. In any case, this issue does not affect the agreement between the experimental and theoretical streamline patterns, since the analytical theory allows for Ekman damping by multiplication the solution with a uniform factor $\exp(-\lambda t)$.

On $\beta at = 4$, however, there is a clear difference between experiment and theory. The experimental flow should have decayed by a factor $\exp(-4/70.7) = 0.945$, but the extremal value 0.35 (we disregard the minus sign) of the stream function in the experiment is smaller than the predicted value $0.49 \times 0.945 = 0.46$. Moreover, the streamlines in the experiment have moved more to the left than in the theory. This difference seems to be connected with the geometrical effect of the sloping bottom. The analytical theory takes the β -effect of the sloping bottom into account, but otherwise the depth is assumed to be

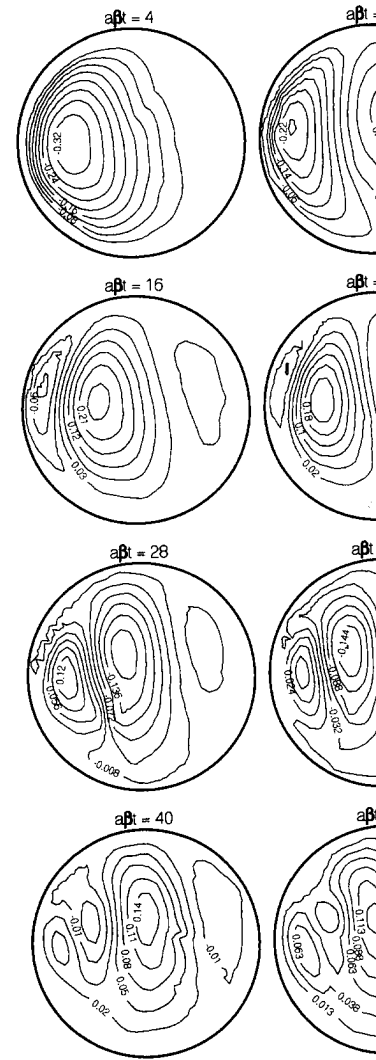


FIGURE 2 Stream function $\psi/\Delta\Omega a^2$ of flow from 10 cm to 20 cm, spin-up from 1.98 to 1.99

uniform; clearly this is not the case. The difference is most pronounced at $t=0$ (not shown). The theoretical solution has circular contours, whereas the experimental flow is

very weak, the accuracy of these results is rather experimental results in this paper. The velocity being an integral over the velocity profile, still gives acceptable results up to $\beta at = 20$, as presented in Figure 2. In spite of the Rossby number value is still noticeable. Around $\beta at = 20$, there is a reflection in the x -axis. This indicates that this is a result of the Rossby number being too large. Moreover, at a closer look, the experimental results seem to evolve slightly faster than the theoretical predictions. However, this can be ascribed to the parameter β in the case of large βat (see Figure 2). As the dimensionless time βat decreases, the speed of the evolution may easily be off

the experiment does not allow a detailed comparison with the theory, but some observations with the stream function can be made. When time becomes weaker than the theoretical prediction, the decay of the experimental flow is faster than the theoretical spin-up time in this experiment is given by $\beta at = 70.7$. This means that at $\beta at = 48$, the flow has decayed by a factor $\exp(-48/70.7) = 0.5$. The experimental and numerical results (see Figure 2, $\beta a \Delta t \approx 4$) shows that this is roughly in agreement. This does not affect the agreement between the experimental streamline patterns, since the analytical streamlines are damped by multiplication the solution with $\exp(-\lambda t)$.

There is a clear difference between experiment and theory. The flow should have decayed by a factor of 0.35 (we disregard the difference in the experiment is smaller than 0.46). Moreover, the streamlines in the experiment are more to the left than in the theory. This is due to the geometrical effect of the sloped bottom. The theory takes the β -effect of the sloped bottom, otherwise the depth is assumed to be

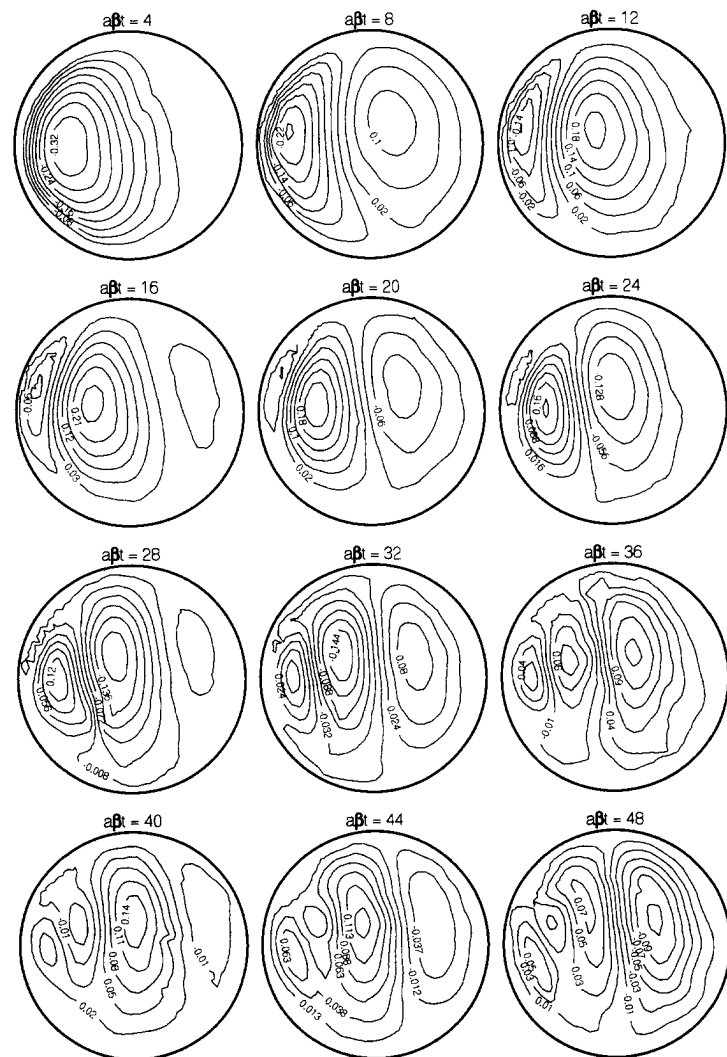


FIGURE 2 Stream function $\psi/\Delta\Omega a^2$ of experiment 1 (radius $a = 20$ cm, depth varying from 10 cm to 20 cm, spin-up from 1.98 to 2.00 rad/s).

uniform; clearly this is not the case in the experiment. This difference is most pronounced at $t = 0$ (not represented in Figs. 1 and 2). The theoretical solution has circular streamlines as initial condition, whereas the experimental flow is asymmetric from the start.

ed differences, from the viewpoint of a
amline pattern, the qualitative agreement
l the theory is striking. Thus, the experi-
confirmation of the analytical results de-
case of the spin-up process.

nts and the numerical simulations will
ues of the Rossby number is considerably
lytical results and the experimental data
is already forecast by an overview of the
e problem. In the theory, time appears
mbination βat , and we use this product
when we present our experimental and
besides the time scale $(\beta a)^{-1}$ one can
on time of the Ekman layer, $(\Delta\Omega)^{-1}$ as
uthal displacement of one radian if the
ationary, $H/(2\sqrt{\nu\Omega})$ as the spin-up time
cale associated with viscous diffusion in
ng facilitates a comparison with the ana-
other aspects of the flow (such as the
ther choices would be more appropriate.

$\nu = 0.1, \kappa = 0.1$

2, with $\Omega = 2$ rad/s, $\Delta\Omega = 0.2$ rad/s, and
cm. With this experiment we exemplify
present more comprehensive results for
xperiments. The experimental data for
are presented in Figures 3 and 4. For
d-body rotation. Then, at about $\beta at = 8$,
sidewall. The vorticity distributions
of cyclonic (dark) vorticity from the
g the formation of the vortex from vor-
at the sidewall. The principal vortex
on grows in size and strength until it
ound $\beta at = 28$, the flow has essentially
rt of the experiment. Later, this struc-
ortex formed in the eastern part of the

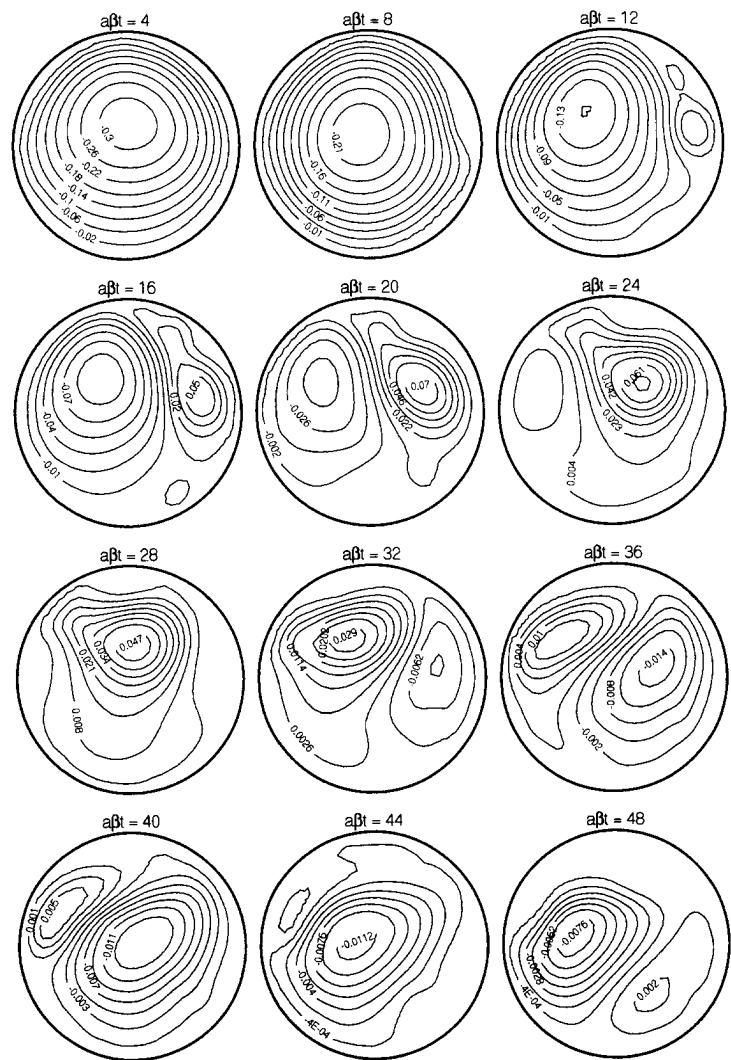


FIGURE 3 Stream function $\psi/\Delta\Omega a^2$ of experiment 2 (radius $a = 20$ cm, depth varying from 18 cm to 20 cm, spin-up from 1.8 to 2.0 rad/s).

In the period from $\beta at = 24$ to 48, the vorticity contours of the shed vortex lose their circular appearance. This is indicative of an increasingly linear behaviour; what one observes is a transition from a strong, nonlinear eddy to a Rossby wave package that is slowly

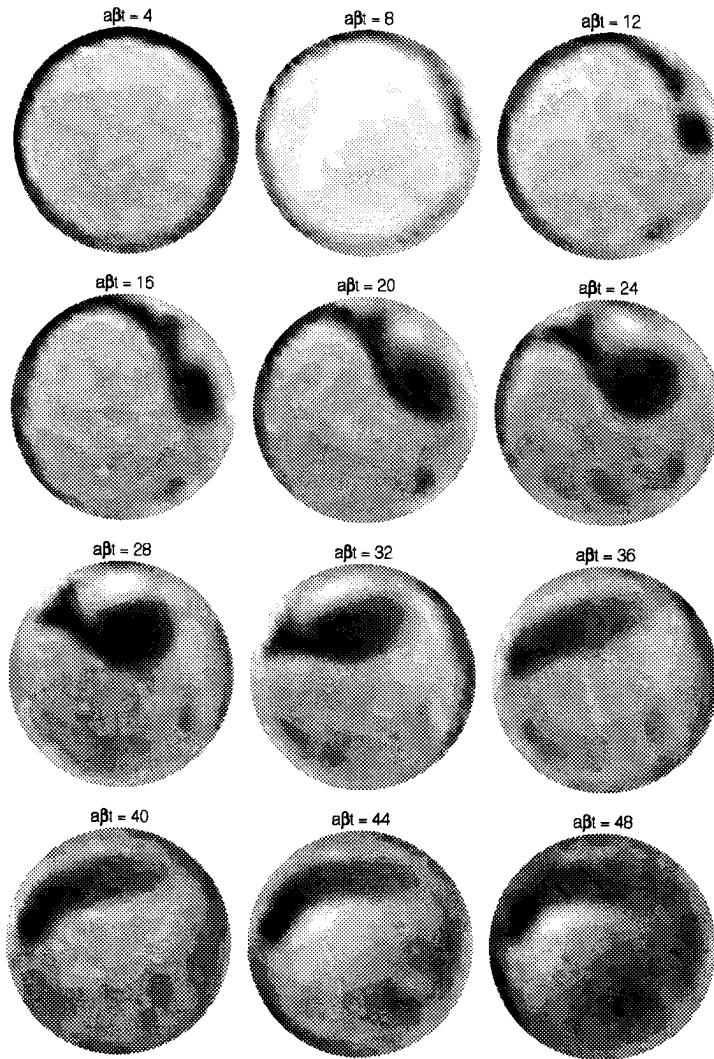


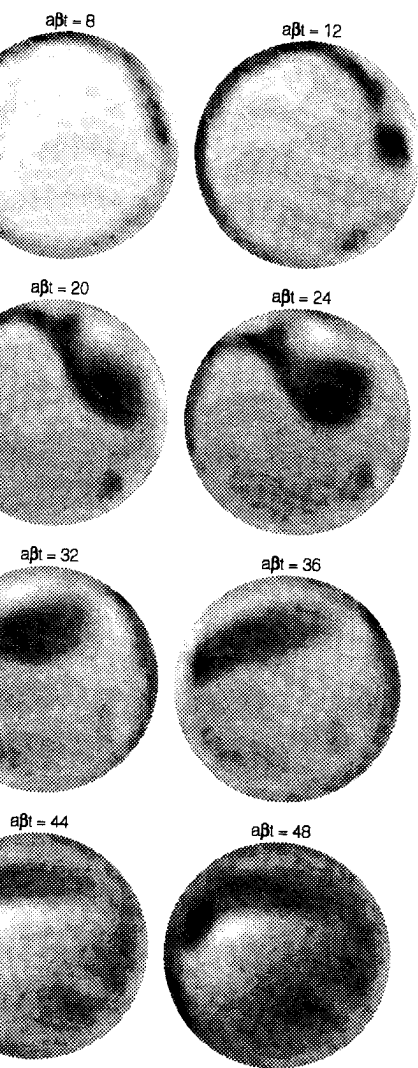
FIGURE 4 Vorticity distribution of experiment 2. The grey scales were chosen to give the best visual impression of the flow, not to facilitate a quantitative comparison between different times. Light corresponds to anticyclonic, dark to cyclonic vorticity. The range of grey scales gradually changes as the relative flow becomes weaker.

dispersed and deformed. The Rossby-wave nature of the flow in later stages can be seen from the general westward motion of the streamline pattern; vortex cells disappear in the western part of the tank, new ones are formed in the eastern part.

6.3. Experiment 3: Spin-down $Ro =$

Experiment 3, spin-down from a bottom elevation of 2 cm, was measured. The basis behind the concept of an in (1): if the fields $\psi(x, y)$, $u(x, y)$, $v(x, y)$ are a solution of (1), then so do $-\psi(x, -y)$, $u(x, -y)$, $v(x, -y)$. Thus, with the parameters β and Ω depending on Ω only, one would expect symmetric results, the symmetry corresponding to the x -axis.

The results for experiment 3 are not perfect, the predicted symmetry is not perfect, the formation of vortices in the eastern part of the tank, the orientation of the separatrix between the two vortices in the eastern part of the experiment are encouraging. In the experimental error; in particular, the results suggest that the flow in the spin-down is faster than in the corresponding spin-up. The question to what extent symmetry is broken. In general, the symmetry between spin-up and spin-down is broken for small Rossby numbers. If the Ekman-damping term in the vorticity equation is unavoidsably breaking the symmetry. In fact, in that case even the spin-down in a circular container with a bottom elevation according to the Wedemeyer mode is not symmetric. In spin-up and spin-down, the Ekman damping term is $\omega/2\Omega\omega$. This leads to cyclonic vortices, which is indeed observed. For $Ro = 0.1$ one could estimate the Ekman damping term in the experiment by $-0.9\lambda\omega$, for $Ro = 0.1$ corresponds to a difference of 2.8 between the spin-up and spin-down stage of the experiment. Since the time lag of the order of 2.8 to correspond with the experimental results, $a\beta/\lambda$ is equal to 14 for this slope. For $a\beta/\lambda = 4$; the streamline patterns for $a\beta/\lambda = 4$ resemble closely those for $a\beta/\lambda$ equal to 14.



periment 2. The grey scales were chosen to give to facilitate a quantitative comparison between cyclonic, dark to cyclonic vorticity. The range relative flow becomes weaker.

ssby-wave nature of the flow in later eral westward motion of the stream- ear in the western part of the tank, ern part.

6.3. Experiment 3: Spin-down $Ro = -0.1$, $\kappa = 0.1$

Experiment 3, spin-down from 2.2 to 2.0 rad/s with a maximal bottom elevation of 2 cm, was meant as the inverse of experiment 2. The basis behind the concept of an 'inverse' experiment is a symmetry in (1): if the fields $\psi(x, y)$, $u(x, y)$, $v(x, y)$ and $\omega(x, y)$ represent a solution of (1), then so do $-\psi(x, -y)$, $u(x, -y)$, $-v(x, -y)$ and $-\omega(x, -y)$. Thus, with the parameters β and ν in (1) held constant and λ depending on Ω only, one would expect experiments 2 and 3 to give symmetric results, the symmetry consisting of a reflection with respect to the x -axis.

The results for experiment 3 are presented in Figure 5. Although not perfect, the predicted symmetry is easy to recognize. In particular, the formation of vortices in the early stage of the experiment and the orientation of the separatrix between large vortices in later stages of the experiment are encouraging. However, the asymmetry is beyond experimental error; in particular, the values of the stream function suggest that the flow in the spin-down experiment decays somewhat faster than in the corresponding spin-up experiment. This raises the question to what extent symmetry-breaking effects can play a role. In general, the symmetry between spin-up and spin-down exists only for small Rossby numbers. If the Rossby number is not small, the Ekman-damping term in the vorticity equation has to be modified, unavoidably breaking the symmetry between spin-up and spin-down. In fact, in that case even the symmetry between spin-up and spin-down in a circular container with a flat bottom would be lost. According to the Wedemeyer model (Wedemeyer, 1964) for nonlinear spin-up and spin-down, the Ekman-suction term is equal to $-\lambda(1 + \omega/2\Omega)\omega$. This leads to cyclonic vortices decaying faster than anticyclonic vortices, which is indeed observed in the experiments. For $Ro = 0.1$ one could estimate the Ekman damping in the beginning of the experiment by $-0.9\lambda\omega$, for $Ro = -0.1$ one finds $-1.1\lambda\omega$. This corresponds to a difference of 20% in the spin-up time in the first stage of the experiment. Since the dimensionless linear spin-up time $a\beta/\lambda$ is equal to 14 for this slope, one would expect a dimensionless time lag of the order of 2.8 to develop. This is in rough agreement with the experimental results, which suggest a time lag of about 4; the streamline patterns for $a\beta t$ equal to 40, 44 and 48 in Figure 3 resemble closely those for $a\beta t$ equal to 36, 40 and 44 in Figure 5.

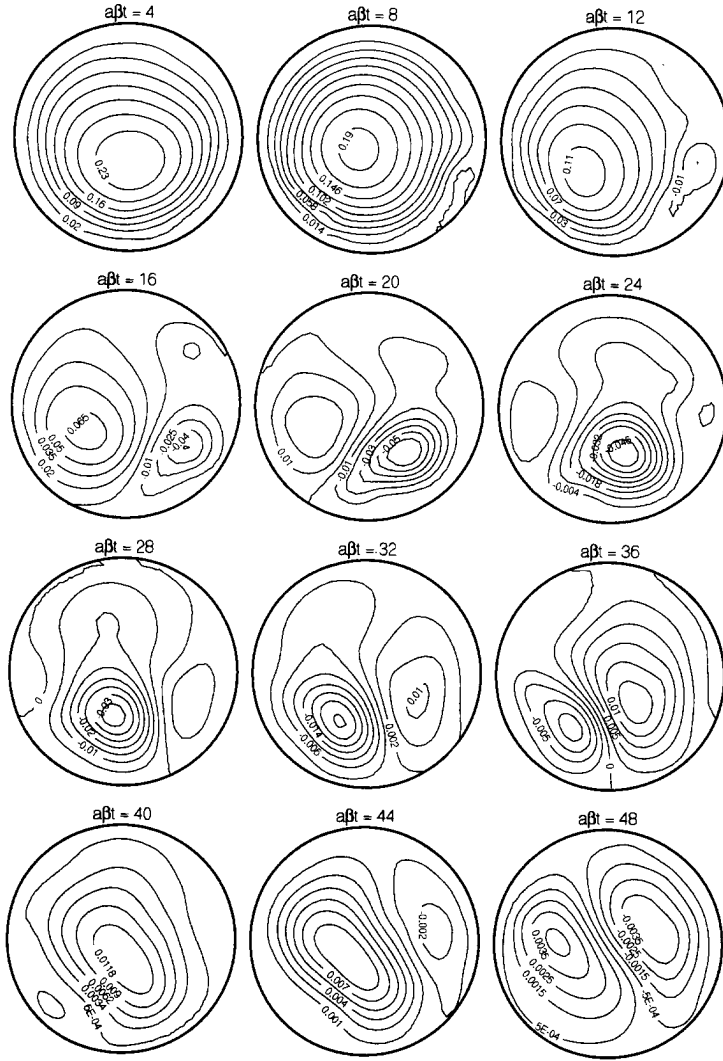


FIGURE 5 Stream function $\psi/\Delta\Omega a^2$ of experiment 3 (radius $a = 20$ cm, depth varying from 18 cm to 20 cm, spin-down from 2.2 to 2.0 rad/s).

6.4. Experiment 4: Spin-up $Ro = 0.1$, $\kappa = 0.5$

The results of experiment 4, in which the topography is again extremely pronounced with the depth varying from 10 to 20 cm, are

represented in Figure 6. Separation a dimensional time measured in seconds fast that we have to allow for an

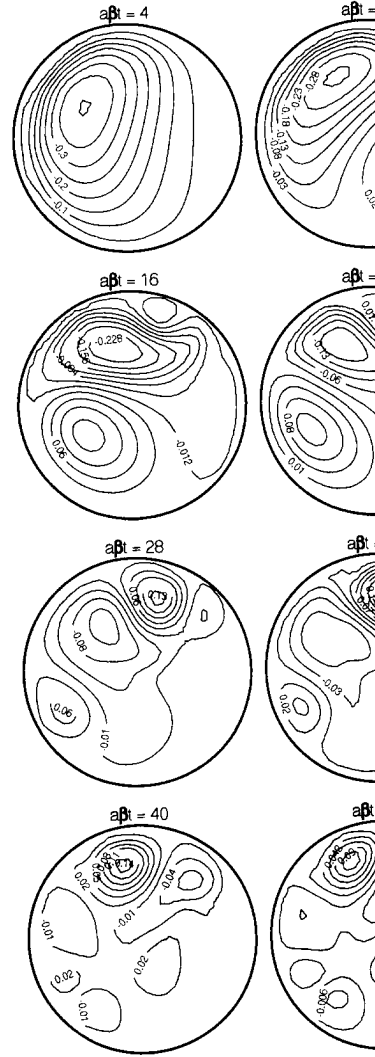
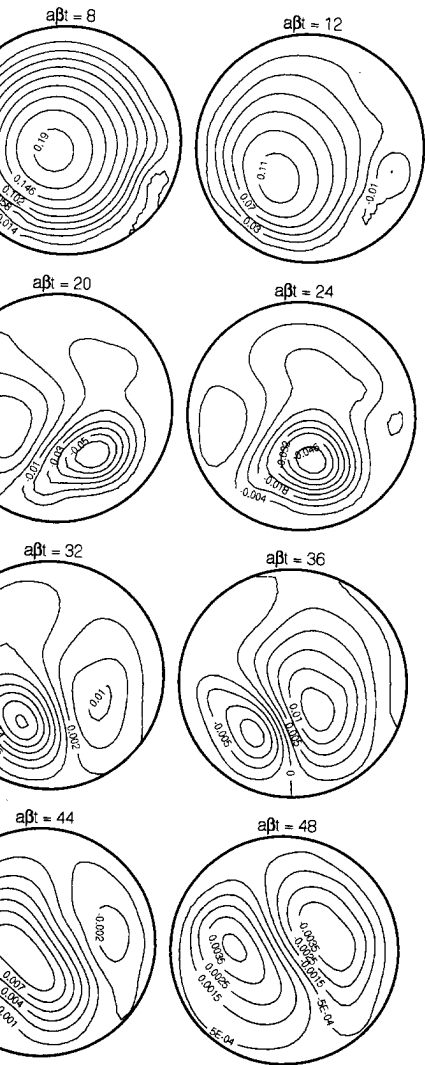


FIGURE 6 Stream function $\psi/\Delta\Omega a^2$ of experiment 4 (radius $a = 20$ cm, depth varying from 10 cm to 20 cm, spin-up from 1.8 to 2.2 rad/s).



of experiment 3 (radius $a = 20$ cm, depth varying from 10 to 20 cm, spin-up from 1.8 to 2.0 rad/s).

$\nu = 0.1$, $\kappa = 0.5$

in which the topography is again depth varying from 10 to 20 cm, are

represented in Figure 6. Separation from the sidewall takes place in a dimensional time measured in seconds. Indeed, the flow evolves so fast that we have to allow for an uncertainty in the reported time

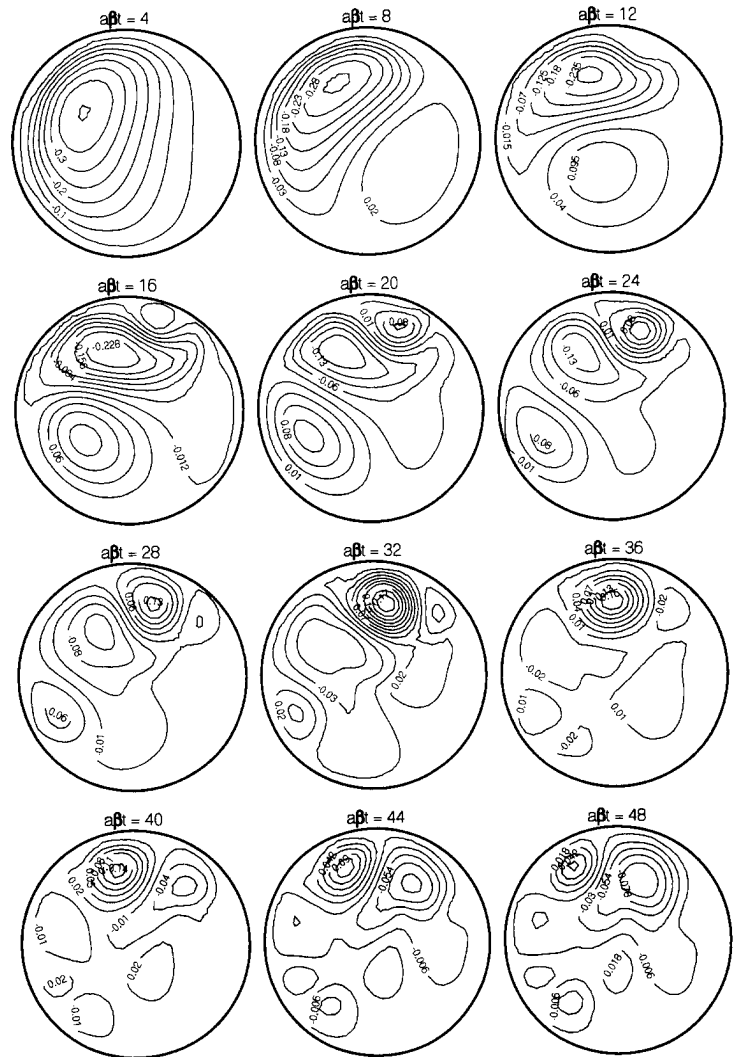


FIGURE 6 Stream function $\psi/\Delta\Omega a^2$ of experiment 4 (radius $a = 20$ cm, depth varying from 10 cm to 20 cm, spin-up from 1.8 to 2.0 rad/s).

of the order of $\beta at = 1$, since it takes several seconds for the table to reach its final angular velocity.

Compared with all other experiments described in this paper, it is striking that experiment 4 shows an anticyclonic rotation of the dipolar structure consisting of the initial anticyclonic cell and the cyclonic cell formed by vortex separation. Again, the only possible explanation for this phenomenon is vortex stretching, caused by the displacement of vortex columns across isobaths; we will return to this matter in the discussion.

In the further evolution of the flow, one can recognize several general properties of the analytical solution that are, at least to a certain extent, also observed in experiments 2 and 3. In the first place, there is a tendency of all vortices to move to the west. This tendency becomes more pronounced as the relative flow becomes weaker. It seems therefore to be plausible that if one would take the streamlines in an advanced stage of the experiment as an initial condition, the analytical model would give a fair description of the flow from that time. Second, the flow is seen to break up into a number of smaller vortices. Unfortunately, the flow decays before really small scales develop. Substituting larger and larger values for βat in the analytical series expression yields a more and more intricate streamline pattern, but as a result of Ekman damping and other experimental limitations we are not able to monitor the flow of experiment 1 for an indefinite time.

7. DISCUSSION OF THE EXPERIMENTAL RESULTS

An important observation in experiments 2, 3 and 4 is vortex shedding from the sidewall in an early stage in the experiment. Vortex shedding consists of the detachment of the initial shear layer from the sidewall, advection of (in the case of spin-up) cyclonic vorticity away from the wall, and the subsequent roll-up into a vortex. This phenomenon is markedly different from the separation and cell formation seen in the analytical results (Fig. 1) and in experiment 1 (Fig. 2). In the analytical results, no sidewall boundary layer with singular vorticity is formed, and no vortex shedding occurs. This is an implication

of the free-slip boundary condition in the analytical model; vortex shedding is caused by the combination of advection and viscous diffusion. If both are present. A further condition for vortex shedding is that the angular displacement in the course of the flow decays on a time scale $\tau = \kappa / \Delta\Omega$ should not be small. For $E \ll 1$ this condition should not be small. For $E \ll 1$ the tiniest increases in angular velocity will cause the fluid elements to move over large distances, but it is another matter whether the spin-up time is not a restriction. If advection and viscous diffusion are absent, the flow depends on the ratio of the advective term and the β -term. If β is small by a typical length scale L and ω is large, the advective term and the β -term are of the same order, which is known as the Rhines length scale. Without dissipation, we may put $L = a$. In the limiting case, the tank is much larger than the Rhines length scale. We can say that $Ro/\kappa = (\Delta\Omega/\Omega)/(\Delta H/a)$ will disrupt the flow after the slightest disturbance. Elements can hardly move without the influence of a field of the same order of magnitude. In the theory, in which $\Delta\Omega/\Omega$ is arbitrary, the flow will be disrupted. In the opposite limit $a/L_{Rh} \ll 1$, the flow in the tank with only slight modifications. The most easily seen by considering a tank with a small slope; the fluid may then rotate with deviations from solid-body rotation.

Additional experiments not reported here are needed to test these conjectures to be valid. In experiment 2, κ and $\Delta\Omega$ are 0.01 and κ decreasing from 0.5 to 0.01, the flow is more circular and the agreement with the analytical results. The value of the Rossby number Ro is a criterion for the theoretical analysis. In experiment 1 and the linear theory, the flow is as to the smallness of the relative

it takes several seconds for the table to
y.

experiments described in this paper, it is
shows an anticyclonic rotation of the
of the initial anticyclonic cell and the
ex separation. Again, the only possible
phenomenon is vortex stretching, caused by the
lines across isobaths; we will return to this

of the flow, one can recognize several
analytical solution that are, at least to a cer-
experiments 2 and 3. In the first place,
vortices to move to the west. This tended
weakened as the relative flow becomes weaker.
possible that if one would take the stream-
the experiment as an initial condition,
give a fair description of the flow from
is seen to break up into a number of
ly, the flow decays before really small
larger and larger values for $\beta a t$ in the
yields a more and more intricate stream-
of Ekman damping and other experi-
able to monitor the flow of experiment

EXPERIMENTAL

experiments 2, 3 and 4 is vortex shed-
early stage in the experiment. Vortex
removal of the initial shear layer from the
case of spin-up) cyclonic vorticity away
ent roll-up into a vortex. This phenom-
from the separation and cell formation
(Fig. 1) and in experiment 1 (Fig. 2).
wall boundary layer with singular vor-
shedding occurs. This is an implication

of the free-slip boundary condition and the missing nonlinearity in
the analytical model; vortex shedding can only take place if both
advection and viscous diffusion (with no-slip boundary condition)
are present. A further condition for vortex shedding is a significant
angular displacement in the course of the spin-up process. Since the
flow decays on a time scale $\tau = H/(2\sqrt{\nu\Omega})$ this means that Ro/\sqrt{E}
should not be small. For $E \ll 1$ this condition is satisfied for all but
the tiniest increases in angular velocity. However, one question is
whether fluid elements have enough time to travel over appreciable
distances, but it is another matter whether they really do so if the finite
spin-up time is not a restriction. Suppose that both Ekman damp-
ing and viscous diffusion are absent. Then, the nature of the time-
dependent flow depends on the ratio between the magnitudes of the
advective term and the β -term. If the flow structures are character-
ized by a typical length scale L and velocity U , then cross-over between
the advective term and the β -term takes place for $L_{Rh} = \sqrt{U/\beta}$,
which is known as the Rhines length scale. In a spin-up experiment
without dissipation, we may put $U = a\Delta\Omega$ and, at the start of the
experiment, $L = a$. In the limiting case $a/L_{Rh} \gg 1$, the radius of the
tank is much larger than the Rhines length scale; equivalently, one
can say that $Ro/\kappa = (\Delta\Omega/\Omega)/(\Delta H/H_{max}) \ll 1$. In this case the β -effect
will disrupt the flow after the slightest spatial displacement; fluid ele-
ments can hardly move without inducing alterations in the velocity
field of the same order of magnitude as the initial flow. The analytical
theory, in which $\Delta\Omega/\Omega$ is arbitrarily small, corresponds to this case.
In the opposite limit $a/L_{Rh} \ll 1$, the fluid may travel all around the
tank with only slight modifications induced by the β -effect. This is
most easily seen by considering a spin-up experiment with a very
small slope; the fluid may then rotate over a full 360° without significant
deviations from solid-body rotation.

Additional experiments not reported in the present paper show
these conjectures to be valid. In particular, in experiments with $Ro =$
0.01 and κ decreasing from 0.5 to 0, the streamlines tend to become
more circular and the agreement with the linear theory is lost. Thus,
the value of the Rossby number being small is really an insufficient
criterion for the theoretical analysis to apply; the agreement between
experiment 1 and the linear theory owes as much to the strong slope
as to the smallness of the relative increase in angular velocity.

Now, consider again the spin-up flow according to the analytical theory. Typical of the solution is the decreasing coherence of the wave modes, resulting in the vortex structures becoming smaller with time. This means that the ratio $L/L_{Rh} \ll 1$ will gradually decrease to the point where the advection can no longer be neglected and the linearity is lost. Note, however, that in the presence of Ekman damping this 'turbulent' stage may never be reached. The Rhines length scale is based on a velocity scale $a\Delta\Omega$, which in the case of Ekman damping should be regarded as an exponentially decreasing quantity. It is therefore possible to perform experiments for which the analytical model (apart from a factor representing the decay of the flow) gives a good representation of the flow at all times. Such a case is shown by experiment 1 (Fig. 2).

It is difficult to give a detailed explanation for when and where the vortex shedding in experiments 2, 3 and 4 (Figs. 3–6) takes place. An elementary consideration is that in the case of spin-up, the shed vortex must be cyclonic, since it consists of the vorticity from the initial shear layer at the wall. Second, one might estimate separation to occur at roughly the same time as in the analytical model, differences appearing by advection of vorticity from the boundary into the interior. However, if $\Delta\Omega/\Omega$ and $\Delta H/H$ are of the same order of magnitude, the separation may occur somewhat later than in the analytical model, since a larger azimuthal displacement is needed to accumulate a change in the relative flow. It seems that this effect is indeed seen in the experiments.

A related issue is the retrograde drift of the shed vortex in experiment 4 (Fig. 6). Apparently, in experiment 4 the value of the parameter Ro/κ is such that the flow is affected strongly by the topography, but only after a rotation of the initial flow over an angle of the order of 180° . Considering the flow as the sum of a solid-body rotation plus a disturbance caused by the vortex stretching, one finds a centre of positive vorticity emerges in the south, and a centre of negative vorticity in the north in that case. Of course, the same topographic vortex stretching is present in experiments 2 and 3, but in that case the disturbance of the relative flow is five times as weak, which is insufficient to disrupt the initial flow within one revolution. On the other hand, if Ro/κ is smaller, the disturbance develops so fast that the vortex-stretching argument applies to small angular

displacements only; this is the point of the analytical theory.

Another aspect of the flow is the point with velocity) in the first fraction of a revolution of the flow field consists of the initial solid-body rotation with the positive lobe in the east. Adding these two contributions, the centre has shifted slightly to the west. This corresponds to the theory of Pedlosky in experiments 2, 3 and 4 the angle is small. After half a revolution ($\Delta\Omega/\Omega$ approximated by a solid-body rotation) the positive lobe in the north and the positive lobe in the south. This corresponds to the observations. Note that the north-south shift of the initial dipole, but is reversed as expressed by the β -term in the

8. NUMERICAL RESULTS

In order to obtain a better understanding of the flow, under consideration, we made a numerical simulation. The parameters corresponding to experiment 1 are used. The stream function and vorticity distributions are shown in Figures 7 and 8. Both the stream function and vorticity distributions show a good agreement between the analytical and numerical data, another indication of the validity of the theory of the flow and the validity of the Ekman layer. However, it is not clear from the figures whether the results are favourable for such a comparison. The topography is moderate, and with $Re = a^2\Delta\Omega/\nu$ of 8000 the flow lies within the range of validity of the numerical code.

Unfortunately, the resolution is not sufficient to give a detailed insight into the flow at early times. The numerical simulation

spin-up flow according to the analytical theory is the decreasing coherence of the wave structures becoming smaller with time. $L_{Rh} \ll 1$ will gradually decrease to the point where it can no longer be neglected and the linear theory is no longer valid in the presence of Ekman damping. A steady state may never be reached. The Rhines length scale L_{Rh} , which in the case of Ekman damping is an exponentially decreasing quantity. It is shown in the experimental results for which the analytical theory (representing the decay of the flow) gives a good description of the flow at all times. Such a case is shown in experiment 4.

A possible explanation for when and where the vortex shedding in experiments 2, 3 and 4 (Figs. 3–6) takes place. It is assumed that in the case of spin-up, the shed vortex consists of the vorticity from the initial dipole. Second, one might estimate separation time as in the analytical model, difference between the time of vorticity from the boundary into the interior. $\Delta\Omega$ and $\Delta H/H$ are of the same order of magnitude. The delay may occur somewhat later than in the case of a steady flow. For azimuthal displacement is needed to separate the shed vortex from the relative flow. It seems that this effect is more pronounced in experiment 4.

In experiment 4 the value of the parameter L_{Rh} is affected strongly by the topography, but the flow is still over an angle of the order of $\pi/2$. The sum of a solid-body rotation plus a dipole, plus vortex stretching, one finds a centre of positive vorticity to the south, and a centre of negative vorticity to the north. Of course, the same topographic effect is present in experiments 2 and 3, but in that case the flow is five times as weak, which is why the vortex shedding occurs within one revolution. On the other hand, the smaller the disturbance develops so much faster. The argument applies to small angular

displacements only; this is the parameter regime described by the analytical theory.

Another aspect of the flow is the position of the centre (i.e., the point with zero velocity) in the first stage of the experiment. After a fraction of a revolution of the flow in the rotating system, the flow field consists of the initial solid-body rotation, plus a weak dipole with the positive lobe in the east and the negative lobe in the west. Adding these two contributions, one finds a velocity field in which the centre has shifted slightly to the west. This conclusion corresponds to the theory of Pedlosky and Greenspan (1967). However, in experiments 2, 3 and 4 the angular displacement does not remain small. After half a revolution ($\Delta\Omega t = \pi$), the velocity field may be approximated by a solid-body rotation, plus a dipole with the negative lobe in the north and the positive lobe in the south. This implies a shift of the centre to the north, in agreement with the experimental observations. Note that the northward shift is not caused by a rotation of the initial dipole, but is really explained by vortex stretching, as expressed by the β -term in the vorticity equation.

8. NUMERICAL RESULTS

In order to obtain a better understanding of the spin-up process under consideration, we made a numerical simulation with the parameters corresponding to experiment 2 (Figs. 2 and 3). The results for the stream function and vorticity of the numerical run are presented in Figures 7 and 8. Both the streamline contour plot and the vorticity distributions show a good agreement between the experimental and numerical data, another indication of the two-dimensional nature of the flow and the validity of the two-dimensional representation of the Ekman layer. However, it should be noted that the conditions are favourable for such a comparison; the Rossby number is small, the topography is moderate, and with a Reynolds number (defined as $Re = a^2 \Delta\Omega / \nu$) of 8000 the flow lies well within the application range of the numerical code.

Unfortunately, the resolution of our experimental method is insufficient to give a detailed insight in the evolution of the flow at early times. The numerical simulations do not have this limitation,

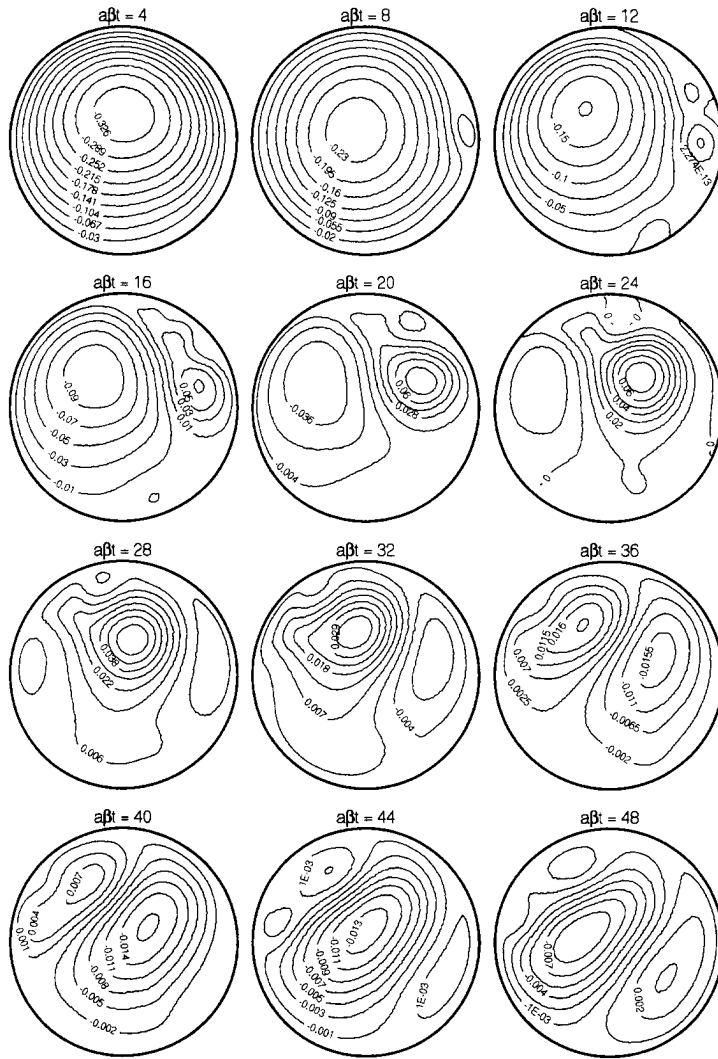


FIGURE 7 Stream function $\psi/\Delta\Omega a^2$ according to the numerical simulation of experiment 2.

and can be used to study the separation and vortex shedding more closely.

First, we determined the separation time, according to the criterion that $\partial v_\theta/\partial r$ be zero at the wall. In order to distinguish between the

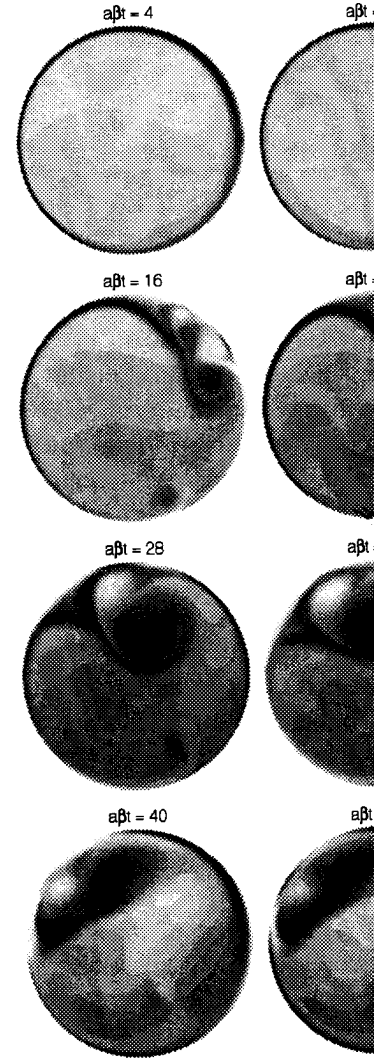


FIGURE 8 Vorticity of the numerical simulation.

influence of different terms in the separation time in three numerical experiments. All three experiments concern Simulation A (the physical run) and

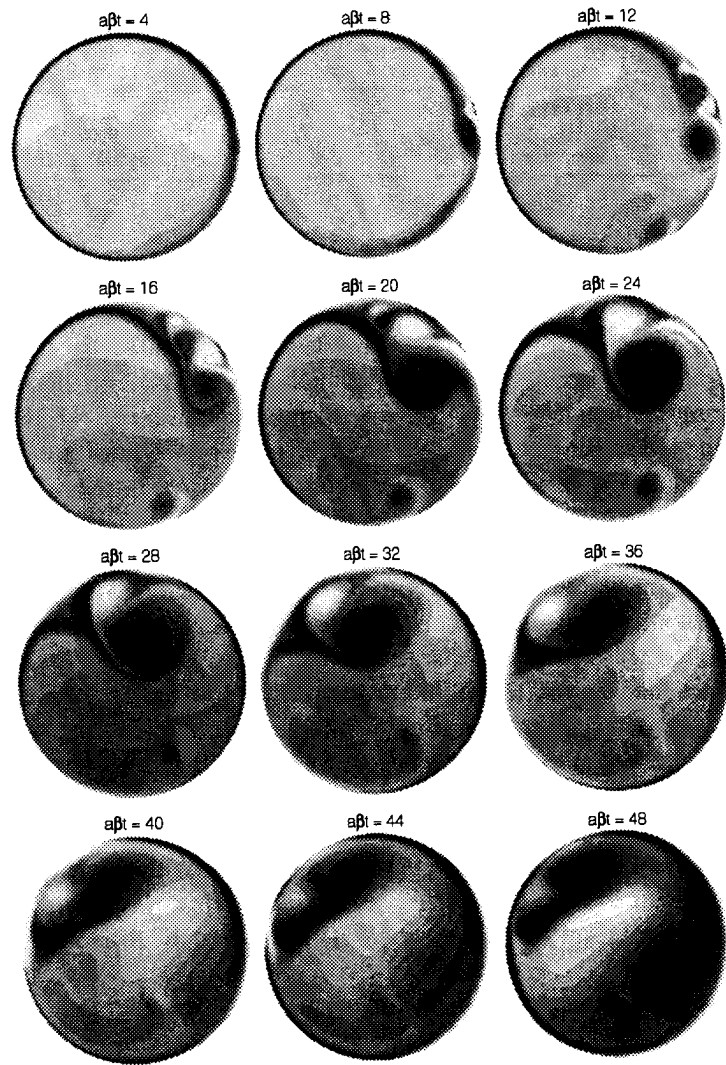
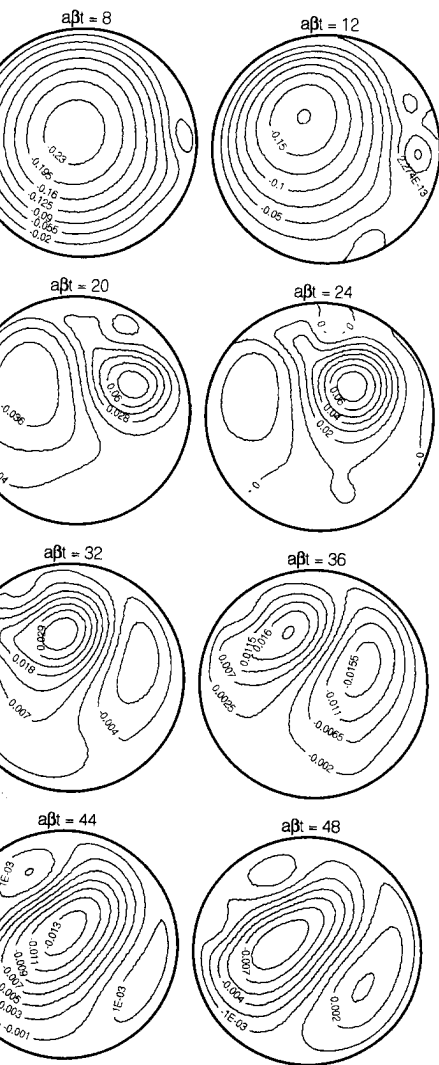


FIGURE 8 Vorticity of the numerical simulation of experiment 2.

Ωa^2 according to the numerical simulation of

the separation and vortex shedding more
separation time, according to the criterion
all. In order to distinguish between the

influence of different terms in the vorticity equation, we calculated the
separation time in three numerical simulations, represented in Table
II. All three experiments concern the parameters of experiment 2.
Simulation A (the physical run) represents the modelling discussed in

TABLE II Numerical simulations with the parameters of experiment 2

	Designation	Diffusion	Advection	Separation time βat_{sep}
Simulation A	Physical run	Yes	Yes	4.19
Simulation B	Inviscid run	No	Yes	8.16
Simulation C	Linear run	No	No	5.69 (analytical model: 5.68)

Sect. 5. In simulation B (the inviscid run), the same parameters are used as in the physical run, but with the diffusive term switched off. In simulation C (the linear run) the advective term is omitted in addition; apart from the uniform damping provided by Ekman pumping, this brings us back to the analytical model. For the physical run we found $\beta at_{sep} = 4.19$, for the inviscid run $\beta at_{sep} = 8.16$ and for the linear run $\beta at_{sep} = 5.69$. The agreement of the linear run with the analytical solution is as expected, and provides a further verification of the correctness of both methods. According to the physical run, the separation time is shorter than in the analytical theory. Apparently, the inward diffusion of positive vorticity accelerates the process of cyclonic vortex formation. The inviscid run indicates that advection tends to delay separation, which is not surprising in view of the fact that the rotating fluid motion will tend to remove concentrations of cyclonic vorticity away from the eastern part of the tank.

Second, we estimated the time at which cyclonic vortices are formed at the sidewall. As a first criterion for the presence of cyclonic vortices, we require the flow to form closed streamlines with $\psi > 0$. In addition, we use a criterion based on the Weiss field (Weiss, 1991), defined as $(1/4)(\sigma^2 - \omega^2)$, with ω the vorticity and $\sigma^2 = (\partial v_x / \partial x - \partial v_y / \partial y)^2 + (\partial v_x / \partial y + \partial v_y / \partial x)^2$ a measure of the strain rate. The Weiss field is required to exceed a somewhat arbitrarily chosen, but very small negative threshold. As a consequence of this second criterion, we find only vortices associated with a local concentration of vorticity, not the vortex cells formed by Rossby-wave propagation. Figure 9 shows the vortex-shedding time *versus* the Rossby number for a number of different values of the slope (non-dimensionalized as $a\beta/\Omega$). For $Ro < 0.05$, we find no separation according to the criteria mentioned above, so the flow is in the Rossby-mode regime. For $0.05 < Ro < 0.1$ a vortex-shedding time is found which is roughly inversely proportional to the Rossby number. This dependence would be in contrast with the analytical theory (according to which the flow field depends on βat only) but is in agreement with the

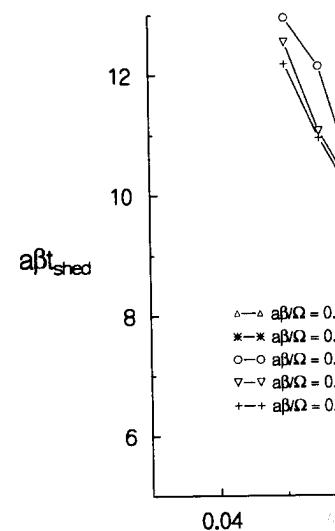


FIGURE 9 Vortex-shedding time according to the criteria mentioned above for spin-up flows with varying Rossby number

notion that for finite Ro/κ and g over a certain angle before the top of the tank. However, this argument also explains the dependence of the vortex-shedding time is, in a reasonable approximation, inversely proportional to the Rossby number. To the extent to which the flow is affected by the number of isobaths that is, a factor two would make the vortex-shedding time short, so the time scale $a\beta t_{shed}$ would

9. CONCLUSION

We have performed four spin-up experiments in a tank with a sloping bottom, all with values of the Rossby number from -0.1 to 0.1 . The results compare well with the results of Pedlosky and Greenspan (1977). Important deviations can occur for $Ro < 0.05$ when the flow seems to meet the criteria on which the vortex-shedding time depends. The flow then departs from an equilibrium between

ulations with the parameters of experiment 2

Diffusion	Advection	Separation time βat_{sep}
Yes	Yes	4.19
No	Yes	8.16
No	No	5.69 (analytical model: 5.68)

the inviscid run), the same parameters are used, but with the diffusive term switched off. In the linear run) the advective term is omitted in the inviscid run) uniform damping provided by Ekman boundary layer is added to the analytical model. For the physical run, for the inviscid run $\beta at_{sep} = 8.16$ and for the linear run $\beta at_{sep} = 5.9$. The agreement of the linear run with the inviscid run is expected, and provides a further verification of both methods. According to the physical theory, the vortex shedding time is shorter than in the analytical theory. The presence of positive vorticity accelerates the vortex formation. The inviscid run indicates that the vortex shedding time is shorter than in the analytical theory, which is not surprising in view of the fact that the vortex shedding time will tend to remove concentration from the eastern part of the tank.

The time at which cyclonic vortices are formed is a criterion for the presence of cyclonic vortices. The criterion is based on the Weiss field (Weiss, $\omega - \omega^2$), with ω the vorticity and $\sigma^2 = -\partial v_y / \partial x^2$ a measure of the strain rate. The criterion is exceeded a somewhat arbitrarily chosen threshold. As a consequence of this second criterion, the vortex shedding time is associated with a local concentration of vorticity formed by Rossby-wave propagation. The vortex shedding time *versus* the Rossby number and the slope of the slope (non-dimensionalized as $a\beta/\Omega$) is shown in Figure 9. For no separation according to the criteria used, the flow is in the Rossby-mode regime. For the linear run, the vortex shedding time is found which is roughly independent of the Rossby number. This dependence is in agreement with the analytical theory (according to which βat_{shed} is only) but is in agreement with the

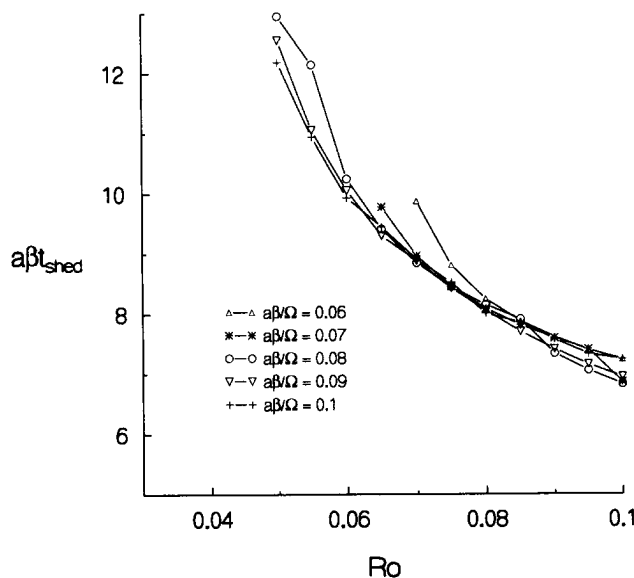


FIGURE 9 Vortex-shedding time according to additional numerical simulations of spin-up flows with varying Rossby number and slope.

notion that for finite Ro/κ and given slope, the fluid has to rotate over a certain angle before the topography becomes noticeable. Moreover, this argument also explains why the scaled vortex-shedding time is, in a reasonable approximation, independent of $a\beta/\Omega$. If the extent to which the flow is affected by the topography is measured by the number of isobaths that is crossed, an increase of the slope by a factor two would make the vortex shedding time twice as short, so the time scale $a\beta t_{shed}$ would be unaltered.

9. CONCLUSION

We have performed four spin-up experiments in a circular tank with a sloping bottom, all with values of the Rossby number in the range from -0.1 to 0.1 . The results confirm the validity of theoretical results of Pedlosky and Greenspan (1967), but also indicate that important deviations can occur for conditions that at first sight would seem to meet the criteria on which the theory is based. The theory departs from an equilibrium between $\partial\omega/\partial t$ and βv_y , and consists of

- Dalziel, S., *DigImage. Image processing for fluid dynamics*, Cambridge Environmental Research Consultants Ltd. (1992).
- Greenspan, H. P., *The Theory of Rotating Fluids*, Cambridge University Press (1968).
- Greenspan, H. P. and Howard, L. N., "On a time-dependent motion in a rotating fluid," *J. Fluid Mech.* **17**, 385 (1963).
- Van Heijst, G. J. F., "Spin-up phenomena in non-axisymmetric containers," *J. Fluid Mech.* **206**, 171 (1989).
- Van Heijst, G. J. F., "Topography effects on vortices in a rotating fluid," *Meccanica* **29**, 431 (1994).
- Van Heijst, G. J. F., Davies, P. A. and Davis, R. G., "Spin-up in a rectangular container," *Phys. Fluids A* **2**(2), 150 (1990).
- Van Heijst, G. J. F., Maas, L. R. M. and Williams, C. W. M., "The spin-up of fluid in a rectangular container with a sloping bottom," *J. Fluid Mech.* **265**, 125 (1994).
- Karniadakis, G. E., Israeli, M. and Orszag, S. A., "High-order splitting methods for the incompressible Navier-Stokes equations," *J. Comp. Phys.* **97**, 414 (1991).
- Van de Konijnenberg, J. A., *Spin-up in non-axisymmetric containers*, Ph.D. Thesis, Eindhoven University of Technology, The Netherlands (1995).
- Van de Konijnenberg, J. A. and Van Heijst, G. J. F., "Nonlinear spin-up in a circular cylinder," *Phys. Fluids* **7**(12), 2989 (1995).
- Nezlin, M. V. and Snezhkin, E. N., *Rossby Vortices, Spiral Structures, Solitons*, Springer, Berlin (1993).
- Pedlosky, J., *Geophysical Fluid Dynamics*, Springer, New York (1987).
- Pedlosky, J. and Greenspan, H. P., "A simple laboratory model for the oceanic circulation," *J. Fluid Mech.* **27**, 291 (1967).
- Rhines, P. B., "Waves and turbulence on a beta-plane," *J. Fluid Mech.* **69**, 417 (1975).
- Suh, Y. K., "Numerical study on two-dimensional spin-up in a rectangle," *Phys. Fluids* **6**(7), 2333 (1994).
- Wedemeyer, E. H., "The unsteady flow within a spinning cylinder," *J. Fluid Mech.* **20**, 383 (1964).
- Weidman, P. D., "On the spin-up and spin-down of a rotating fluid," *J. Fluid Mech.* **77**, 685 (1976).
- Weiss, J., "The dynamics of enstrophy transfer in two-dimensional hydrodynamics," *Physica D* **48**, 273 (1991).

ON THE NORMAL MODE OF HARMONIC ON A SPHERE

YU. N. S.

*Centro de Ciencias de la Atmósfera
 de México, Circuito Exterior, CU*

(Received 26 May 1999; In final form ...)

The normal mode instability of harmonic wave on a rotating sphere is analytically studied. By polynomial flow $\alpha P_n(\mu)$ ($n \geq 1$) and steady rotation H_n is the subspace of homogeneous spherical harmonics of order n . F_1 is the one-dimensional subspace generated by the normal mode instability. A necessary condition for the normal mode instability is derived. By this condition, Fjørtoft's (1953) average energy theorem is shown to be necessary for an unstable mode must be equal to $\sqrt{n(n+1)}$ (and hence, exponentially and algebraically growing) wavenumber m satisfies condition $|m| \geq n$. The normal modes are estimated as well. It is shown that the normal modes are unstable, decaying or non-stationary mode.

The new instability condition can be used to a harmonic wave and on trials of normal mode instability of Legendre-polynomial flow, it complements the latter while the latter is related to the basic flow structure of a growing perturbation.

Keywords: Normal mode instability; Legendre-polynomial flow; wave

1. INTRODUCTION

In this paper we consider the normal mode instability of a Legendre-polynomial (LP) flow

*Tel.: (525) 622-4247, Fax: (525) 622-4090